CLEO CONF 02-07
ICHEP02 ABS949

Study of Two-Photon Transitions in CLEO-III $\Upsilon(3S)$ Data*

D. Cinabro,[1] M. Dubrovin,[1] S. McGee,[1] A. Bornheim,[2] E. Lipeles,[2] S. P. Pappas,[2] A. Shapiro,[2] W. M. Sun,[2] A. J. Weinstein,[2] R. Mahapatra,[3] R. A. Briere,[4] G. P. Chen,[4] T. Ferguson,[4] G. Tatishvili,[4] H. Vogel,[4] N. E. Adam,[5] J. P. Alexander,[5] K. Berkelman,[5] V. Boisvert,[5] D. G. Cassel,[5] P. S. Drell,[5] J. E. Duboscq,[5] K. M. Ecklund,[5] R. Ehrlich,[5] R. S. Galik,[5] L. Gibbons,[5] B. Gittelman,[5] S. W. Gray,[5] D. L. Hartill,[5] B. K. Heltsley,[5] L. Hsu,[5] C. D. Jones,[5] J. Kandaswamy,[5] D. L. Kreinick,[5] A. Magerkurth,[5] H. Mahlke-Krüger,[5] T. O. Meyer,[5] N. B. Mistry,[5] E. Nordberg,[5] J. R. Patterson,[5] D. Peterson,[5] J. Pivarski,[5] D. Riley,[5] A. J. Sadoff,[5] H. Schwarthoff,[5] M. R. Shepherd,[5] J. G. Thayer,[5] D. Urner,[5] G. Viehhauser,[5] A. Warburton,[5] M. Weinberger,[5] S. B. Athar,[6] P. Avery,[6] L. Breva-Newell,[6] V. Potlia,[6] H. Stoeck,[6] J. Yelton,[6] G. Brandenburg,[7] D. Y.-J. Kim,[7] R. Wilson,[7] K. Benslama,[8] B. I. Eisenstein,[8] J. Ernst,[8] G. D. Gollin,[8] R. M. Hans,[8] I. Karliner,[8] N. Lowrey,[8] C. Plager,[8] C. Sedlack,[8] M. Selen,[8] J. J. Thaler,[8] J. Williams,[8] K. W. Edwards,[9] R. Ammar,[10] D. Besson,[10] X. Zhao,[10] S. Anderson,[11] V. V. Frolov,[11] Y. Kubota,[11] S. J. Lee,[11] S. Z. Li,[11] R. Poling,[11] A. Smith,[11] C. J. Stepaniak,[11] J. Urheim,[11] Z. Metreveli,[12] K.K. Seth,[12] A. Tomaradze,[12] P. Zweber,[12] S. Ahmed,[13] M. S. Alam,[13] L. Jian,[13] M. Saleem,[13] F. Wappler,[13] E. Eckhart,[14] K. K. Gan,[14] C. Gwon,[14] T. Hart,[14] K. Honscheid,[14] D. Hufnagel,[14] H. Kagan,[14] R. Kass,[14] T. K. Pedlar,[14] J. B. Thayer,[14] E. von Toerne,[14] T. Wilksen,[14] M. M. Zoeller,[14] H. Muramatsu,[15] S. J. Richichi,[15] H. Severini,[15] P. Skubic,[15] S.A. Dytman,[16] J.A. Mueller,[16] S. Nam,[16] V. Savinov,[16] S. Chen,[17] J. W. Hinson,[17] J. Lee,[17] D. H. Miller,[17] V. Pavlunin,[17] E. I. Shibata,[17] I. P. J. Shipsey,[17] D. Cronin-Hennessy,[18] A.L. Lyon,[18] C. S. Park,[18] W. Park,[18] E. H. Thorndike,[18] T. E. Coan,[19] Y. S. Gao,[19] F. Liu,[19] Y. Maravin,[19] R. Stroynowski,[19] M. Artuso,[20] C. Boulahouache,[20] K. Bukin,[20] E. Dambasuren,[20] K. Khroustalev,[20] R. Mountain,[20] R. Nandakumar,[20] T. Skwarnicki,[20] S. Stone,[20] J.C. Wang,[20] A. H. Mahmood,[21] S. E. Csorna,[22] and I. Danko[22]

(CLEO Collaboration)

[1] *Wayne State University, Detroit, Michigan 48202*
[2] *California Institute of Technology, Pasadena, California 91125*
[3] *University of California, Santa Barbara, California 93106*
[4] *Carnegie Mellon University, Pittsburgh, Pennsylvania 15213*
[5] *Cornell University, Ithaca, New York 14853*
[6] *University of Florida, Gainesville, Florida 32611*
[7] *Harvard University, Cambridge, Massachusetts 02138*
[8] *University of Illinois, Urbana-Champaign, Illinois 61801*
[9] *Carleton University, Ottawa, Ontario, Canada K1S 5B6*
and the Institute of Particle Physics, Canada M5S 1A7
[10] *University of Kansas, Lawrence, Kansas 66045*
[11] *University of Minnesota, Minneapolis, Minnesota 55455*
[12] *Northwestern University, Evanston, Illinois 60208*
[13] *State University of New York at Albany, Albany, New York 12222*
[14] *Ohio State University, Columbus, Ohio 43210*
[15] *University of Oklahoma, Norman, Oklahoma 73019*
[16] *University of Pittsburgh, Pittsburgh, Pennsylvania 15260*

[17]*Purdue University, West Lafayette, Indiana 47907*
[18]*University of Rochester, Rochester, New York 14627*
[19]*Southern Methodist University, Dallas, Texas 75275*
[20]*Syracuse University, Syracuse, New York 13244*
[21]*University of Texas - Pan American, Edinburg, Texas 78539*
[22]*Vanderbilt University, Nashville, Tennessee 37235*
(Dated: July 23, 2002)

Abstract

We have studied two-photon transitions from $\Upsilon(3S)$ decays recorded by the CLEO-III detector in exclusive events with two photons and either two electrons or two muons. We obtain precision measurements of the $\chi_b(2P_J)$ masses for $J = 2$ and $J = 1$. The transition rates for all three spin states of the $2P$ triplet are measured with improved precision which leads to a better determination of their hadronic width ratios. We also observe rare transitions via the $\chi_b(1P)$ states. The measured rates for these transitions allow a determination of $< 1P|r|3S >$, the E1 matrix element, which is more sensitive to the structure of the $b\bar{b}$ states than the $< 2P|r|3S >$ matrix element which dominates the radiative decays of the $\Upsilon(3S)$ state.

We also present first upper limits on the branching ratios for $\Upsilon(3S) \to \pi^0\Upsilon(2S)$, $\Upsilon(3S) \to \pi^0\Upsilon(1S)$ and a new limit for the branching ratio for $\Upsilon(3S) \to \eta\Upsilon(1S)$.

*Submitted to the 31st International Conference on High Energy Physics, July 2002, Amsterdam

I. INTRODUCTION

Long-lived $b\bar{b}$ states are especially well suited for testing QCD via lattice calculations [1] and effective theories of strong interactions, like potential models [2].

In this paper we analyze events with two photons and two leptons (two electrons or two muons). The events are constrained to be consistent with the $\Upsilon(3S) \to \gamma\gamma\Upsilon(2S)$ or $\Upsilon(3S) \to \gamma\gamma\Upsilon(1S)$ transitions, with the $\Upsilon(2S)$ or $\Upsilon(1S)$ decaying to a lepton pair. The analysis of similar events containing four photons and two leptons is the subject of a separate paper submitted to this conference [4].

The various photon transitions that contribute to our data are outlined in Fig. 1. The two-photon sample is dominated by photon transitions from the $\Upsilon(3S)$ to one of the triplet $\chi_b(2P_J)$ states, followed by a subsequent photon transition to the $\Upsilon(2S)$ or $\Upsilon(1S)$. The product branching ratios for these decays can be unfolded using the known measurements for $\mathcal{B}(\chi_b(2P_J) \to \gamma\Upsilon(2S))$ or $\mathcal{B}(\chi_b(2P_J) \to \gamma\Upsilon(1S))$. The ratios of these branching fractions for the same J and different final state Υ test theoretical predictions for the ratio of the corresponding E1 matrix elements, $|<2S|r|2P>|/|<1S|r|1P>|$. Ratios of these branching fractions for different J and the same final state Υ give us insight into the ratios of the hadronic widths of the various $\chi_b(2P_J)$ states. Measurement of the photon energies in the first transition allows a mass determination of the $\chi_b(2P)$ states.

We also observe the rare photon cascade $\Upsilon(3S) \to \gamma\chi_b(1P_J)$, $\chi_b(1P) \to \gamma\Upsilon(1S)$. From the measured product branching ratio, we derive the $<1P|r|3S>$ E1 matrix element, which is of particular interest since different theoretical estimates of its value disagree.

We also use our sample to search for π^0 and η transitions between the $\Upsilon(3S)$ and either the $\Upsilon(2S)$ or $\Upsilon(1S)$. The π^0 transitions are isospin violating decays. Analogous transitions were previously observed in the $c\bar{c}$ system between the $\psi(2S)$ and $J/\psi(1S)$ [5].

The two-photon cascade transitions via the P states were previously observed by the CUSB [6] and CLEO-II [7] experiments. Here, we present the results based on 1.1 fb^{-1} of integrated luminosity accumulated at the $\Upsilon(3S)$ resonance, corresponding to $4.73 \cdot 10^6$ $\Upsilon(3S)$ decays. This is roughly a ten-fold increase in statistics compared to the CLEO-II data set, and roughly a four-fold increase compared to the integrated CUSB data set. Thanks to the good granularity and large solid angle of the CLEO CsI(Tl) calorimeter, the CLEO-III detection efficiency for these final states is a factor of 2-3 larger than in the CUSB detector. Even though the CLEO-III calorimeter is essentially the same as in the CLEO-II detector [8], the photon selection efficiency and detector resolution were improved in the endcaps and in part of the barrel calorimeter thanks to a new, lower-mass, tracking system [9] built for CLEO-III. Another change was the replacement of the time-of-flight system by a RICH detector in the barrel part. Finally, the calorimeter endcaps were restacked and moved farther away from the interaction point to accommodate a new, higher luminosity, interaction point optics.

II. DATA SELECTION

We select events with exactly two photons and two oppositely charged leptons. The leptons must have momenta of at least 3.75 GeV. We distinguish between electrons and muons by their energy deposition in the calorimeter. Electrons must have a high ratio of energy observed in the calorimeter to the momentum measured in the tracking system ($E/p > 0.7$). Muons are identified as minimum ionizing particles, and are required to

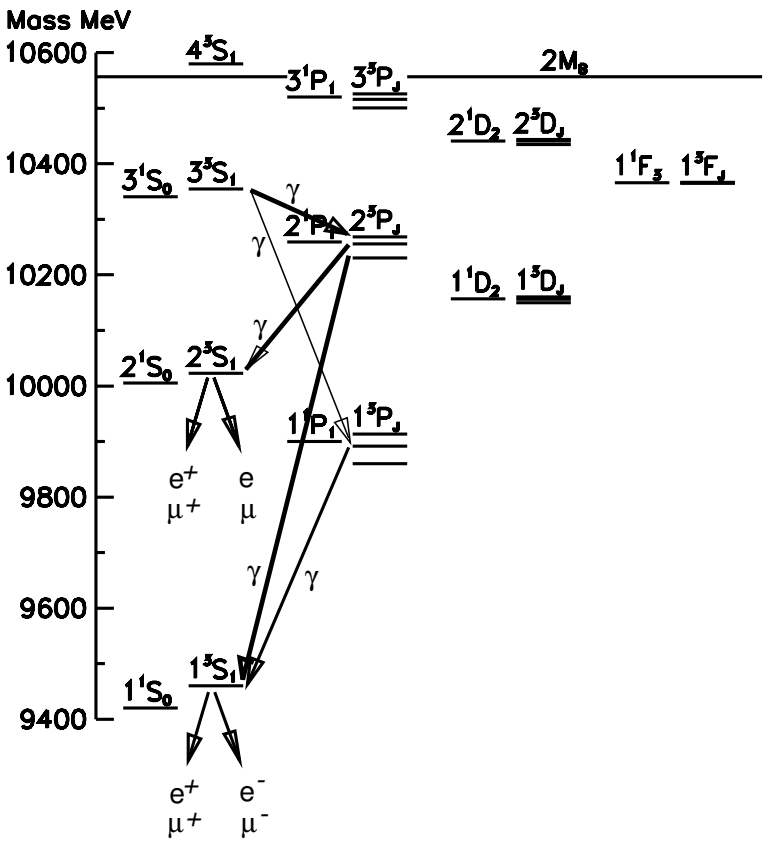

FIG. 1: $b\bar{b}$ mass levels as predicted by one of the potential models. The levels are denoted by their spectroscopic labels, $n^{2S+1}L_J$, where n is the radial quantum number ($n = 1, 2, \ldots$), S is the total quark spin ($S = 0$ spin singlets, $S = 1$ spin triplets), L is the orbital angular momentum ($L = S, P, D, \ldots$) and J is the total angular momentum of the state ($\vec{J} = \vec{S} + \vec{L}$). Two-photon transition sequences via the $\chi_b(2P)$ or $\chi_b(1P)$ states are indicated.

leave $150 - 550$ MeV of energy in the calorimeter. Stricter muon identification does not reduce the background in the final sample, since all significant background sources contain muons. Each photon must have at least 60 MeV of energy. We also ignore all photons below 180 MeV in the calorimeter region closest to the beam, because of the spurious photons generated by beam-related backgrounds. The total momentum of all photons and leptons in each event must be balanced to within 300 MeV. The invariant mass of the two leptons must be consistent with either the $\Upsilon(1S)$ or $\Upsilon(2S)$ mass within ± 300 MeV. Much better identification of the $\Upsilon(1S)$ or $\Upsilon(2S)$ resonance is obtained by measuring the mass of the system recoiling against the two photons. The average resolution of the recoil mass is 15 MeV (9 MeV) for the $\Upsilon(1S)$ ($\Upsilon(2S)$). The resolution of the different states in the $\chi_b(2P)$ triplet relies on the energy measurement of the lower energy photon in the event. This photon must be detected in the barrel part of the calorimeter, where the energy resolution is best. The higher energy photon is allowed to be detected in the endcap part for the $\gamma\gamma\mu^+\mu^-$ events.

The final discrimination against the backgrounds is performed by using the energy of the lower energy photon and the mass of the system recoiling against the photons. The energy of the less energetic photon, $E_{\gamma\,low}$, must peak for the signal events at one of the values

corresponding to $(M^2_{\Upsilon(3S)} - M^2_{\chi_b(2,1P_J)})/(2\,M_{\Upsilon(3S)})$ for various J. The recoil mass, M_{recoil}, calculated using the photon four-vectors and the beam energy, must peak at the $\Upsilon(2S)$ or $\Upsilon(1S)$ mass. We actually use the difference between the center-of-mass energy and the mass of the system recoiling against the photons, $\Delta M = E_{CM} - M_{recoil}$, which peaks at $M_{\Upsilon(3S)} - M_{\Upsilon(2,1S)}$ for the signal events. Scatter plots of ΔM versus $E_{\gamma\,low}$ are shown for $\mu^+\mu^-$ and e^+e^- events separately in Figs. 2-3. Clusters of events for $\Upsilon(3S) \to \gamma\chi_b(2P_{2,1})$ followed by a radiative decay to the $\Upsilon(2S)$ or $\Upsilon(1S)$ are clearly visible. A less intense cluster of events, corresponding to $\Upsilon(3S) \to \gamma\chi_b(1P_{2,1})$, $\chi_b(1P_{2,1}) \to \gamma\Upsilon(1S)$, is also visible. The backgrounds vary smoothly over these two variables and come predominantly from radiative Bhabhas and $\mu-$pair events. The e^+e^- channel clearly has much higher background due to the higher Bhabha cross-section.

III. MASS DETERMINATION FOR THE $\chi_b(2P_{2,1})$ STATES

To determine the masses of the $\chi_b(2P)$ states, we combine the data for the two-photon cascades to the $\Upsilon(2S)$ and the $\Upsilon(1S)$. The recoil mass difference ΔM must be within $\pm 3\sigma$ of the expected value. The energy spectrum of the lower energy photon is plotted in Fig. 4.

From the three photon lines expected from $\Upsilon(3S) \to \gamma\chi_b(2P_{2,1,0})$ transitions, only the $J = 2$ and $J = 1$ lines are clearly visible. The third $J = 0$ line is suppressed by the larger hadronic width of this state, which makes its radiative branching ratios small. In the fit to the data (see Fig. 4), we parameterize each line by a Gaussian with an asymmetric low-energy tail. The number of events and the peak energy for each line are free parameters in the fit, except for the position of the $J = 0$ line, which was fixed to the value obtained from the fit to the inclusive photon spectrum in multi-hadronic events. The ratios of the widths of the three peaks were fixed to the Monte Carlo determined dependence of the energy resolution on the photon energy. The overall energy resolution scale factor was left free in the fit. We also fixed the energy dependence of the turn-over point from the Gaussian to the power-law tail from the Monte Carlo simulations. Again, an overall scaling factor for the turn-over point was adjusted to the data by the fit. The backgrounds were assumed to be linear in energy, as suggested by the ΔM sidebands, the off-resonance data (0.13 fb^{-1} collected below the $\Upsilon(3S)$ resonance) and other data taken at the $\Upsilon(4S)$. The fit yields 1286 ± 63 events for the $J = 2$ line positioned at 86.1 ± 0.3 MeV, 2726 ± 180 events for the $J = 1$ line positioned at 99.1 ± 0.2 MeV and 45 ± 34 events for the $J = 0$ line. The fitted energy resolution scale factor is 1.05 ± 0.03, thus the data are consistent with the Monte Carlo simulations. The fitted energy resolution corresponds to $\sigma_{E_\gamma} = (4.6 \pm 0.2)$ MeV for $E_\gamma = 100$ MeV.

Splitting the data into di-electron and di-muon subsamples, as well as $\Upsilon(2S)$ and $\Upsilon(1S)$ subsamples, gives consistent results within the statistical errors. Varying the order of the background polynomial and the fit range results in very small changes to the fitted photon energies. The dominant systematic error is due to the uncertainties in fixing the absolute photon energy scale at various photon energies. We used $\pi^0 \to \gamma\gamma$ decays and the known π^0 mass to correct for small non-linearities in the shower energy determination. Then, we used the recoil mass distributions in the $\Upsilon(3S) \to \gamma\gamma\Upsilon(2S)$ and $\Upsilon(3S) \to \gamma\gamma\Upsilon(1S)$ data presented here, as well as the $\Upsilon(3S) \to \pi^0\pi^0\Upsilon(2S)$ and $\Upsilon(3S) \to \pi^0\pi^0\Upsilon(1S)$ transitions, together with the well known $\Upsilon(1S)$, $\Upsilon(2S)$, $\Upsilon(3S)$ masses [5], to check the π^0 calibration. From this study we have determined our systematic uncertainty in the photon energies relevant for the $J = 2, 1$ lines to be 0.35%.

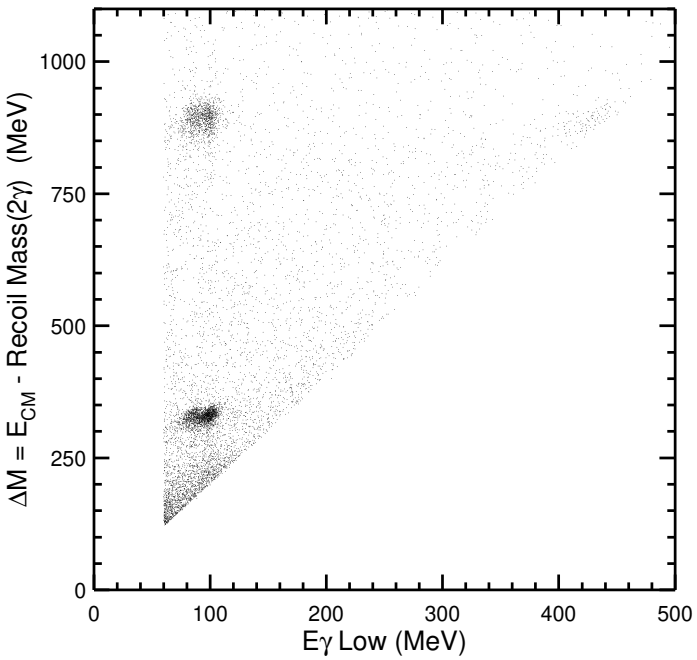

FIG. 2: The center-of-mass energy minus the mass of the system recoiling against the two photons (ΔM) vs. the energy of the less energetic photon for $\gamma\gamma\mu^+\mu^-$ events. The two clusters of events correspond to $\Upsilon(3S) \to \gamma\chi_b(2P)$ ($E_{\gamma\,low} \sim 90$ MeV) followed by either $\chi_b(2P) \to \gamma\Upsilon(2S)$ ($\Delta M \sim 330$ MeV) or $\chi_b(2P) \to \gamma\Upsilon(1S)$ ($\Delta M \sim 895$ MeV). A faint cluster of events corresponding to $\Upsilon(3S) \to \gamma\chi_b(1P)$, $\chi_b(1P) \to \gamma\Upsilon(1S)$ ($E_{\gamma\,low} \sim 410$ MeV, $\Delta M \sim 895$ MeV), is also visible.

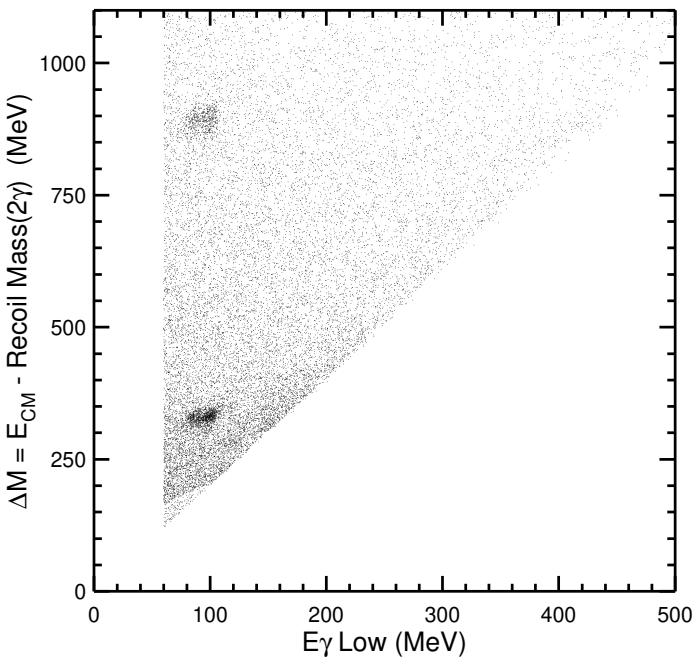

FIG. 3: Similar plot for $\gamma\gamma e^+e^-$ events.

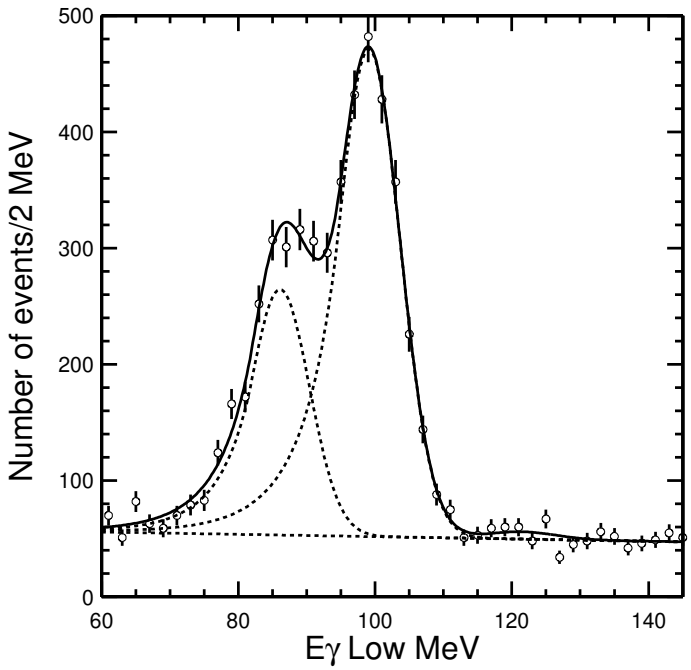

FIG. 4: Energy of the less energetic photon in $\Upsilon(3S) \to \gamma\gamma l^+ l^-$ events. The two large peaks correspond to $\Upsilon(3S) \to \gamma\chi_b(2P_2)$ and $\Upsilon(3S) \to \gamma\chi_b(2P_1)$ transitions. There is also an insignificant peak at an energy corresponding to $\Upsilon(3S) \to \gamma\chi_b(2P_0)$. The solid line represents the fit. The dashed lines show the fitted background (linear function) and the two individual photon lines on top of the background.

Including the systematic error (strongly correlated between the two lines), the photon energies are:

$$E_{J=2} = (86.09 \pm 0.30 \pm 0.29)\,\mathrm{MeV},$$
$$E_{J=1} = (99.08 \pm 0.17 \pm 0.34)\,\mathrm{MeV}.$$

These results are consistent with, but more precise than, previous determinations [5].

Using the $\Upsilon(3S)$ mass [5], we can turn these photon-line energies into $\chi_b(2P_{2,1})$ masses:

$$M_{\chi_b(2P_2)} = (10268.8 \pm 0.3 \pm 0.6)\,\mathrm{MeV},$$
$$M_{\chi_b(2P_1)} = (10255.6 \pm 0.2 \pm 0.6)\,\mathrm{MeV}.$$

IV. BRANCHING RATIOS FOR PHOTON CASCADES VIA THE $\chi_b(2P)$ STATES

We can determine the product branching ratios for the cascade sequence from the photon-line amplitudes fitted separately to the $\Upsilon(2S)$ and $\Upsilon(1S)$ subsamples. The efficiency for each photon line was determined from Monte Carlo simulations that included the full angular correlations between the photons and leptons [10]. We also simulated final state radiation in the annihilation to lepton pairs [11]. In addition to one-dimensional fits to the $E_{\gamma\,low}$ distributions, we also performed two-dimensional fits to ΔM vs. $E_{\gamma\,low}$ which improved the

statistical errors. The systematic errors were determined from variations of the cuts, and the fit procedure and from the uncertainty in the number of $\Upsilon(3S)$ decays in our sample. After we determine the product branching ratios for $\mathcal{B}(\Upsilon(3S) \to \gamma\gamma l^+l^-)$, we also unfold them for $\mathcal{B}(\Upsilon(3S) \to \gamma\gamma\Upsilon(2,1S))$ using the world average values for $\mathcal{B}(\Upsilon(2,1S) \to l^+l^-)$ [12], and finally, for $\mathcal{B}(\chi_b(2P_J) \to \gamma\Upsilon(2,1S))$ using the world average values for $\mathcal{B}(\Upsilon(3S) \to \gamma\chi_b(2P_J))$ [5]. All the results are summarized in Table I, which also contains a comparison with previous measurements. The statistical significance of the $J = 0$ signal for the $\Upsilon(3S) \to \gamma\gamma\Upsilon(2S)$ transitions is three standard deviations (see Table I). Since the $J = 0$ amplitude for the $\Upsilon(3S) \to \gamma\gamma\Upsilon(1S)$ transition is less significant (2.5σ), we do not claim observation of this transition and set an upper limit on its rate at the 90% confidence level. Our results are generally in agreement with previous measurements, except for the cascade rates via the $\chi_b(2P_1)$ state, for which we (and the previous CLEO-II analysis) measure a substantially higher rate than obtained by CUSB. In all cases, our measurements have better precision than the previous determinations.

V. BRANCHING RATIOS FOR PHOTON CASCADES VIA THE $\chi_b(1P)$ STATES

For $\Upsilon(3S) \to \gamma\chi_b(1P)$, $\chi_b(1P) \to \gamma\Upsilon(1S)$ transitions, the first and second photons have similar energies. Furthermore, the photon energies of the $J = 2$ and $J = 1$ lines cannot be resolved with our energy resolution. Therefore, the $E_{\gamma\,low}$ variable is no longer useful. In this channel, we measure the sum of the branching fractions for all the J states. The $J = 0$ contribution is expected to be small since it is suppressed by the large hadronic width of this state. To obtain a signal amplitude, we fit the $\Delta' M/\sigma(\Delta M)$ distribution, where $\Delta' M = \Delta M - (M_{\Upsilon(3S)} - M_{\Upsilon 1S})$, after requiring $E_{\gamma\,high} - E_{\gamma\,low} < 100$ MeV. While for di-electron events both photons are required to be in the barrel region of the calorimeter, for di-muon events one photon is allowed in the endcaps. In the fits, the signal shape was determined from Monte Carlo events. The fits are displayed in Figs. 5-6 and the results are tabulated in Table II. The systematic error were determined from variations of the cuts, and the fit procedure and from the uncertainty in the number of $\Upsilon(3S)$ decays in our sample.

VI. SEARCH FOR π^0 AND η TRANSITIONS

To search for $\Upsilon(3S) \to \pi^0\Upsilon(2S)$, $\Upsilon(3S) \to \pi^0\Upsilon(1S)$ and $\Upsilon(3S) \to \eta\Upsilon(1S)$ transitions, we use the same sample of events as for the studies of the two-photon transitions described above. To suppress the two-photon transitions, we require $E_{\gamma\,low} > 135$ MeV and $E_{\gamma\,high} - E_{\gamma\,low} > 100$ MeV for the $\Upsilon(1S)$ subsample, and $E_{\gamma\,low} > 115$ MeV for the $\Upsilon(2S)$ subsample. For $\Upsilon(3S) \to \pi^0\Upsilon(2S)$ [$\Upsilon(3S) \to \eta\Upsilon(1S)$] we require the two-photon recoil mass to be within 3 standard deviations of the $\Upsilon(2S)$ [$\Upsilon(1S)$] mass, and look for a π^0 [η] mass peak in the distribution of $(M_{\gamma\gamma} - M_{\pi^0})/\sigma(M_{\gamma\gamma})$ [$(M_{\gamma\gamma} - M_\eta)/\sigma(M_{\gamma\gamma})$], where $\sigma(M_{\gamma\gamma})$ is the expected mass resolution for a given $\gamma\gamma$ pair. The signal is expected to be nearly the standard Gaussian (mean close to zero and $\sigma \approx 1$) in these variables. No such peaks are observed in the data, as shown in Figs. 7-8. From the fit of a signal contribution on top of a polynomial background, we obtain upper limits on the number of observed signal events. For the $\Upsilon(3S) \to \pi^0\Upsilon(1S)$ candidates, the backgrounds peak sharply below the π^0 mass, as shown in Fig. 9, which makes it difficult to fit this distribution for a signal peak. Therefore, instead we first require $-1 < (M_{\gamma\gamma} - M_{\pi^0})/\sigma(M_{\gamma\gamma}) < +3$ and then plot the π^0 recoil mass

TABLE I: Rate results for $\Upsilon(3S) \to \gamma\chi_b(2P_J) \to \gamma\gamma\Upsilon(2,1S) \to \gamma\gamma l^+l^-$. $\mathcal{B}(\gamma\gamma l^+l^-)$ means an average of $\mathcal{B}(\gamma\gamma\mu^+\mu^-)$ and $\mathcal{B}(\gamma\gamma e^+e^-)$. The first error is statistical and second (if given) is systematic. CLEO-II and CUSB measurements for $\mathcal{B}(\gamma\gamma l^+l^-)$ are also given for comparison. Upper limits are at the 90% C.L.

	$J=2$		$J=1$		$J=0$	
	$\mu\mu$	ee	$\mu\mu$	ee	$\mu\mu$	ee
$\Upsilon(3S) \to \Upsilon(2S)$						
Number of events	483±32	291±30	1081±39	697±36	$30.3^{+11.0}_{-10.1}$	$21.0^{+17.4}_{-16.4}$
Efficiency (%)	36.5±0.4	23.7±0.4	38.2±0.4	26.3±0.4	39.3±0.4	23.7±0.4
$\mathcal{B}(\gamma\gamma l^+l^-)$ in 10^{-4} CLEO-III	2.73±0.15±0.24		5.84±0.17±0.41		0.17±0.06±0.02	
CLEO-II [7]	2.49±0.47±0.31		5.11±0.60±0.63		<0.60	
CUSB [6]	2.74±0.33±0.18		3.30±0.33±0.19		0.40±0.17±0.03	
$\mathcal{B}(\Upsilon(3S) \to \gamma\gamma\Upsilon(2S))$ in 10^{-2} CLEO-III	2.20±0.12±0.31		4.69±0.14±0.62		0.14±0.05±0.02	
$\mathcal{B}(\chi_b(2P) \to \gamma\Upsilon(2S))$ in 10^{-2} CLEO-III	19.3±1.1±3.1		41.5±1.2±5.9		2.59±0.92±0.51	
$\Upsilon(3S) \to \Upsilon(1S)$						
Number of events	353±25	186±23	587±28	370±26	$18.0^{+7.7}_{-6.8}$	$7.8^{+11.9}_{-10.8}$
Efficiency (%)	36.4±0.6	24.8±0.6	37.9±0.6	25.7±0.6	39.9±0.6	27.6±0.6
$\mathcal{B}(\gamma\gamma l^+l^-)$ in 10^{-4} CLEO-III	1.93±0.12±0.17		3.19±0.13±0.18		< 0.16	
CLEO-II [7]	2.51±0.47±0.32		3.24±0.56±0.41		<0.32	
CUSB [6]	1.98±0.28±0.12		2.34±0.28±0.14		0.13±0.10±0.03	
$\mathcal{B}(\Upsilon(3S) \to \gamma\gamma\Upsilon(1S))$ in 10^{-2} CLEO-III	0.79±0.05±0.07		1.31±0.05±0.08		<0.08	
$\mathcal{B}(\chi_b(2P) \to \gamma\Upsilon(1S))$ in 10^{-2} CLEO-III	7.0±0.4±0.8		11.6±0.4±0.9		<1.44	

distribution (see Fig. 10). The backgrounds are smooth in this variable. Again, no signal peak is observed and we set an upper limit on the number of signal events. The systematic error in the efficiency determination and the signal extraction is found to be 20%. We increase the upper limits on the branching ratios by 20% to account for this uncertainty. The results are summarized in Table III.

TABLE II: Results for $\Upsilon(3S) \to \gamma\chi_b(1P_J) \to \gamma\gamma\Upsilon(1S) \to \gamma\gamma l^+l^-$ summed over all the J states. The first error is statistical and second (if given) is systematic. A CUSB measurement is also shown for comparison.

	$\mu\mu$	ee
Number of events	118±13	49±13
Efficiency (%)	45.4±0.4	28.8±0.3
$\mathcal{B}(\Upsilon(3S) \to \gamma\gamma l^+l^-)$ in 10^{-4} CLEO-III	0.520±0.054±0.052	
$\mathcal{B}(\Upsilon(3S) \to \gamma\gamma\Upsilon(1S))$ in 10^{-2} CLEO-III	0.214±0.022±0.021	
CUSB [6]	0.12±0.04±0.01	

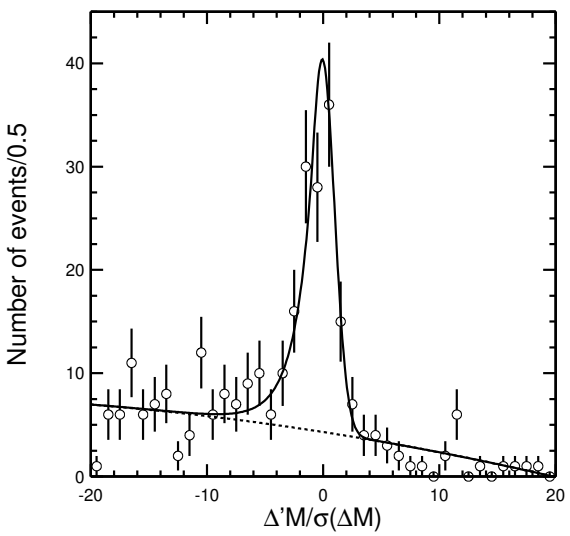

FIG. 5: The $\Delta' M/\sigma(\Delta M)$ distribution for $\gamma\gamma\mu^+\mu^-$ events. The solid line represents the fit. The dashed line shows the fitted background.

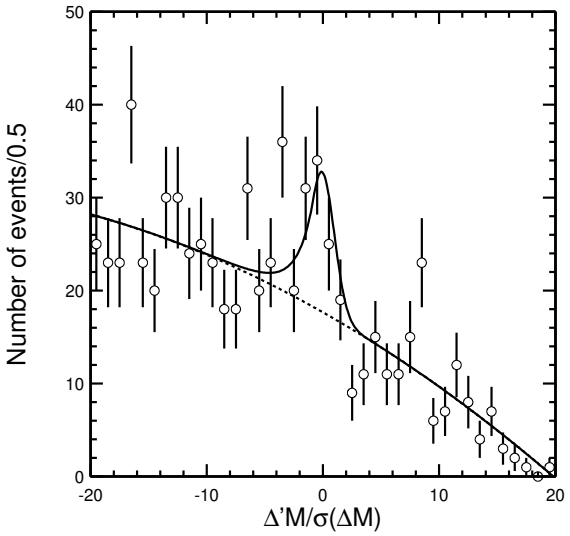

FIG. 6: The $\Delta' M/\sigma(\Delta M)$ distribution for $\gamma\gamma e^+e^-$ events.

VII. COMPARISON OF THE TWO-PHOTON TRANSITION RESULTS TO THEORY

A. E1 matrix elements

The $\mathcal{B}(\Upsilon(3S) \to \gamma\gamma\Upsilon(2,1S))$ via $\chi_b(2P)$ and $\chi_b(1P)$ states measured here can be compared to potential model predictions for the E1 matrix elements in two ways. First, the ratio of the magnitudes of the matrix elements for the decay of the same $\chi_b(2P_J)$ state to

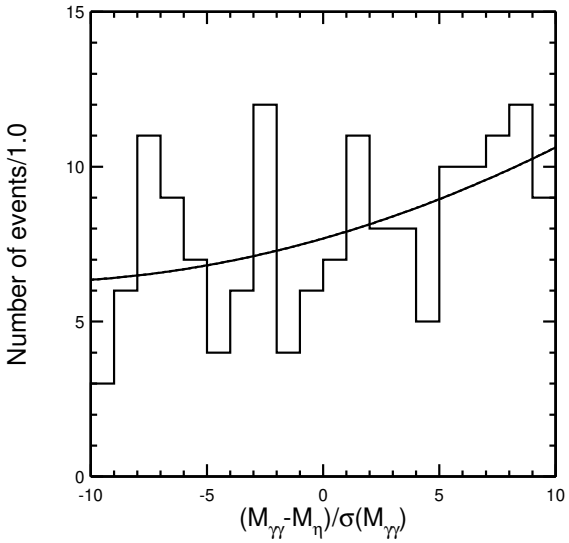

FIG. 7: The deviation of the two-photon invariant mass from the η mass for $\Upsilon(3S) \to \gamma\gamma\Upsilon(1S)$ events. The solid line represents the fit. The number of signal events from the fit is zero.

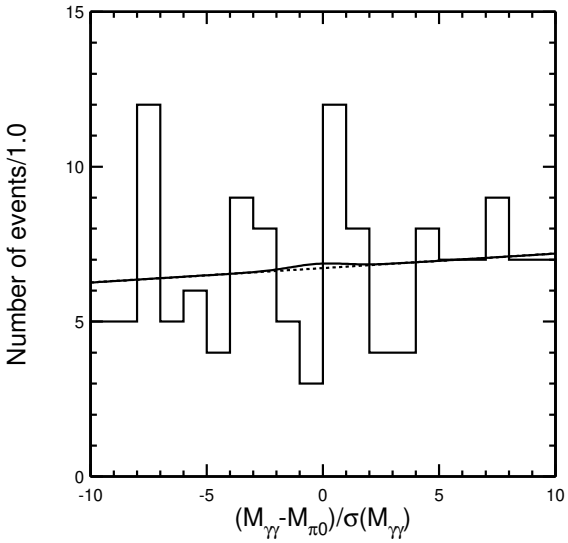

FIG. 8: The deviation of the two-photon invariant mass from the π^0 mass for $\Upsilon(3S) \to \gamma\gamma\Upsilon(2S)$ events. The solid line represents the fit. The dashed line represents the fitted background alone.

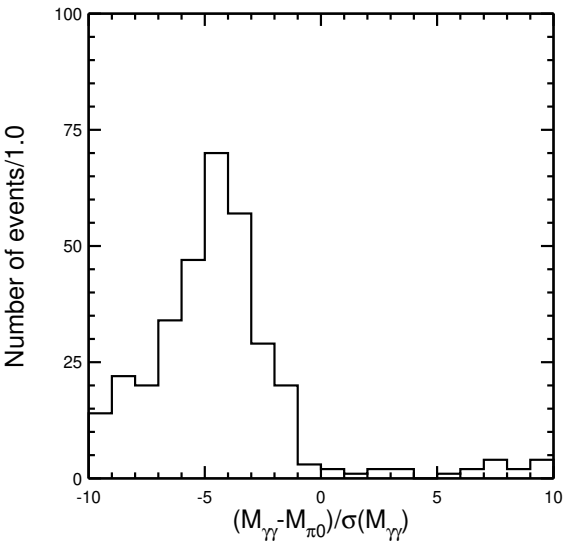

FIG. 9: The deviation of the two-photon invariant mass from the π^0 mass for $\Upsilon(3S) \to \gamma\gamma\Upsilon(1S)$ events.

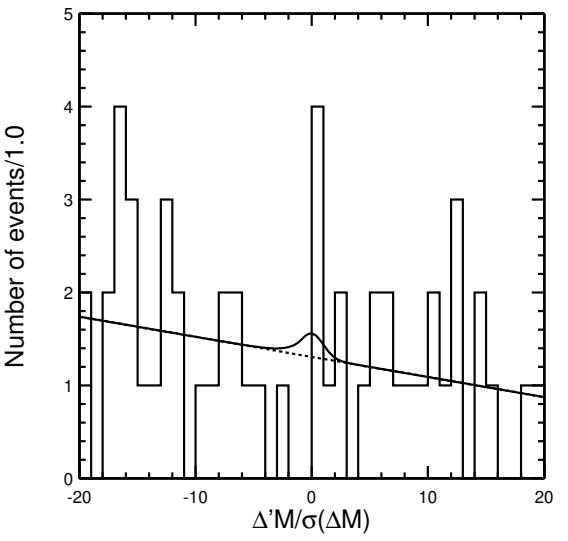

FIG. 10: The recoil mass deviation from the $\Upsilon(1S)$ mass for $\Upsilon(3S) \to \gamma\gamma\Upsilon(1S)$ events. The solid line represents the fit. The dashed line represents the fitted background alone.

TABLE III: Results for $\Upsilon(3S) \to \pi^0\Upsilon(1S)$, $\Upsilon(3S) \to \eta\Upsilon(1S)$, $\Upsilon(3S) \to \pi^0\Upsilon(2S)$ transitions. The efficiency quoted for the η transition excludes $\mathcal{B}(\eta \to \gamma\gamma)$ [5].

	$\Upsilon(3S) \to \pi^0\Upsilon(1S)$	$\Upsilon(3S) \to \eta\Upsilon(1S)$	$\Upsilon(3S) \to \pi^0\Upsilon(2S)$
# of signal events	$0.7^{+2.8}_{-0.7}$	$0.0^{+3.5}_{-0.0}$	$0.4^{+6.5}_{-0.4}$
90% C.L. U.L. on signal events	< 5.3	< 6.0	< 11.0
efficiency (%)	16.5 ± 0.4	8.9 ± 0.3	9.7 ± 0.3
90% C.L. U.L. on $\mathcal{B}(\pi^0/\eta l^+l^-)$	$< 0.41 \cdot 10^{-5}$	$< 2.2 \cdot 10^{-5}$	$< 1.5 \cdot 10^{-5}$
90% C.L. U.L. on $\mathcal{B}(\pi^0/\eta)$	$< 0.17 \cdot 10^{-3}$	$< 0.90 \cdot 10^{-3}$	$< 1.2 \cdot 10^{-3}$
previous U.L. on $\mathcal{B}(\eta)$ [25]	—	$< 2.2 \cdot 10^{-3}$	—

different S states can be obtained from:

$$\frac{|<2P_J|r|1S>|}{|<2P_J|r|2S>|} = \sqrt{\frac{\mathcal{B}(3S \to \gamma 2P_J, 2P_J \to \gamma 1S)}{\mathcal{B}(3S \to \gamma 2P_J, 2P_J \to \gamma 2S)} \left(\frac{E_\gamma(2P_J \to 2S)}{E_\gamma(2P_J \to 1S)}\right)^3},$$

where $E_\gamma(2P_J \to 1, 2S)$ can be obtained from the well known masses of the initial and final states [5]. Using the branching ratios given in Table I, we obtain:

$$\begin{aligned}
\tfrac{|<2P_2|r|1S>|}{|<2P_2|r|2S>|} &= 0.105 \pm 0.004 \pm 0.006, \\
\tfrac{|<2P_1|r|1S>|}{|<2P_1|r|2S>|} &= 0.087 \pm 0.002 \pm 0.005, \\
\tfrac{|<2P_2|r|1S>|}{|<2P_2|r|2S>|} \Big/ \tfrac{|<2P_1|r|1S>|}{|<2P_1|r|2S>|} &= 1.21 \pm 0.06, \\
\tfrac{|<2P_{2,1}|r|1S>|}{|<2P_{2,1}|r|2S>|} &= 0.096 \pm 0.002 \pm 0.005,
\end{aligned}$$

where the first error is due to the statistical uncertainties in the radiative branching ratios and the second error is due to the uncertainties in $\mathcal{B}(\Upsilon(1,2S) \to l^+l^-)$ (thus, we assume that all other systematics cancel). In the non-relativistic limit, the E1 matrix elements do not depend on J. Since our results for $J = 2$ and $J = 1$ differ by 3.5 standard deviations, we conclude that there is evidence for relativistic effects. To compare to the potential model prediction, we calculated an average over $J = 2$ and $J = 1$ (the fourth result above).

We can also extract the $|<1P|r|3S>|$ matrix element from the photon transitions via the $\chi_b(1P)$ states:

$$|<1P|r|3S>| = \sqrt{\frac{\mathcal{B}(3S \to \gamma 1P, 1P \to \gamma 1S)\,\Gamma_{tot}(3S)}{D\,\sum_J (2J+1) E_\gamma(1P_J \to 1S)^3 \mathcal{B}(1P_J \to \gamma 1S)}},$$

where $D = 4/27\,\alpha\,{e_b}^3 = 1.2 \cdot 10^{-4}$ (α is the fine structure constant, and e_b is the $b-$quark electric charge). This formula assumes that the matrix element is spin independent. Taking

TABLE IV: Comparison of E1 matrix elements and their ratios predicted by different potential models with measurements from $b\bar{b}$ data. "NR" denotes non-relativistic calculations and "rel" refers to models with relativistic corrections.

	$\lvert<2P\lvert r\rvert3S>\rvert$		$\lvert<1P\lvert r\rvert2S>\rvert$		$\lvert<1P\lvert r\rvert3S>\rvert$		$\frac{\lvert<1S\lvert r\rvert2P>\rvert}{\lvert<2S\lvert r\rvert2P>\rvert}$	
	GeV^{-1}		GeV^{-1}		GeV^{-1}			
DATA	2.7±0.2		1.9±0.2		0.050±0.006		0.096±0.005	
	World Average				This measurement			
Model	NR	rel	NR	rel	NR	rel	NR	rel
Kwong, Rosner [13]	2.7		1.6		0.023		0.13	
Fulcher [14]	2.6		1.6		0.023		0.13	
Büchmuller et al.[15]	2.7		1.6		0.010		0.12	
Moxhay, Rosner [16]	2.7	2.7	1.6	1.6	0.024	0.044	0.13	0.15
Gupta et al.[17]	2.6		1.6		0.040		0.11	
Gupta et al.[18]	2.6		1.6		0.010		0.12	
Fulcher [19]	2.6		1.6		0.018		0.11	
Danghighian et al.[20]	2.8	2.5	1.7	1.3	0.024	0.037	0.13	0.10
McClary, Byers [21]	2.6	2.5	1.7	1.6			0.15	0.13
Eichten et al.[22]	2.6		1.7		0.110		0.15	
Grotch et al.[23]	2.7	2.5	1.7	1.5	0.011	0.061	0.13	0.19

$\mathcal{B}(3S \to \gamma 1P, 1P \to \gamma 1S)$ from Table II and the world average values for the other quantities [5], we obtain:

$$|<1P|r|3S>| = (0.050 \pm 0.006)\, GeV^{-1}\,.$$

The error here includes the statistical and systematic uncertainties on all quantities added in quadrature.

These results are compared to various potential model predictions in Table IV. We also include a comparison between various potential model predictions and experimental results for $|<2P|r|3S>|$ and $|<1P|r|2S>|$ extracted from the world average results for $B(\Upsilon(3S) \to \gamma\chi_b(2P_J))$ and $B(\Upsilon(2S) \to \gamma\chi_b(1P_J)$ (taken from Ref. [3]).

While most of the potential models have no trouble reproducing the large matrix elements, $|<2P|r|3S>|$, $|<1P|r|2S>|$, which show also little model dependence, only a few models predict $|<1P|r|3S>|$ in agreement with our measurement. Clearly, the latter transition is more sensitive to the underlying description of $b\bar{b}$ states. Predictions for the ratio $\frac{|<2P|r|1S>|}{|<2P|r|2S>|}$ are not as model dependent, but somewhat higher than our experimental value.

B. Ratio of hadronic widths of the $\chi_b(2P_J)$ states

Assuming spin independence of the matrix elements, the ratios of hadronic widths ($\Gamma_{had} = \Gamma_{tot} - \Gamma_{E1}$) of the $\chi_b(2P_J)$ states can be derived from:

$$\frac{\Gamma_{had}(2P_{Ja})}{\Gamma_{had}(2P_{Jb})} = \left(\frac{E_\gamma(2P_{Ja} \to 2S)}{E_\gamma(2P_{Jb} \to 2S)}\right)^3 \frac{1/\mathcal{B}(2P_{Ja} \to \gamma 2S) - 1}{1/\mathcal{B}(2P_{Jb} \to \gamma 2S) - 1} \quad .$$

Taking $\mathcal{B}(2P_{Ja} \to \gamma 2S)$ from Table I and applying this formula to $Ja = 0$ and $Jb = 2$, we obtain:

$$\frac{\Gamma_{had}(2P_0)}{\Gamma_{had}(2P_2)} = 5.6 \pm 2.6.$$

To leading order in perturbative QCD, both states annihilate to two hard gluons and the ratio is expected to be simply the ratio of spin counting factors: 15/4=3.75 [24]. However, QCD correction are known to be large. Thus, there is rough agreement between the data and the expectations. A more precise determination of $\mathcal{B}(2P_0 \to \gamma 2S)$ would be useful.

The $J = 1$ state cannot annihilate to two massless gluons. Thus, to leading order in perturbative QCD, the hadronic width of the $2P_1$ state is suppressed by one power of the strong coupling constant. The data confirm this suppression:

$$\frac{\Gamma_{had}(2P_1)}{\Gamma_{had}(2P_2)} = 0.29 \pm 0.06.$$

VIII. SUMMARY

We have presented improved measurements of the photon energies in $\Upsilon(3S) \to \gamma\chi_b(2P_2)$ and $\Upsilon(3S) \to \gamma\chi_b(2P_1)$. We have also produced improved measurements of the product branching ratios for $\Upsilon(3S) \to \gamma\gamma\Upsilon(2S)$ and $\Upsilon(3S) \to \gamma\gamma\Upsilon(1S)$ proceeding through the $\chi_b(2P_J)$ states (measured for each J separately), and proceeding through the $\chi_b(1P_J)$ states (measured as a sum for $J = 2, 1$).

Finally, we have determined upper limits on the branching ratios for $\Upsilon(3S) \to \pi^0\Upsilon(2S)$, $\Upsilon(3S) \to \pi^0\Upsilon(1S)$, and $\Upsilon(3S) \to \eta\Upsilon(1S)$, the first two of which were obtained for the first time.

We gratefully acknowledge the effort of the CESR staff in providing us with excellent luminosity and running conditions. M. Selen thanks the PFF program of the NSF and the Research Corporation, and A.H. Mahmood thanks the Texas Advanced Research Program. This work was supported by the National Science Foundation, and the U.S. Department of Energy.

[1] See e.g. C. T. Davies *et al.* (UKQCD Collaboration), Phys. Rev. D **58**, 054505 (1998) and references therein.
[2] For a review see: E. Eichten and C. Quigg, Phys. Rev. **D49**, 5845 (1994) and Ref. [3].
[3] D. Besson and T. Skwarnicki, Ann. Rev. Nucl. Part. Sci. **43**, 333 (1993).
[4] "First Observation of $\Upsilon(1D)$ States", CLEO Collaboration, paper submitted to this conference. S. E. Csorna *et al.* (CLEO), paper submitted to this conference, ICHEP02 ABS948, CLEO CONF 02-06.
[5] K. Hagiwara *et al.* (Particle Data Group) Phys. Rev. **D66**, 010001 (2002).
[6] U. Heintz *et al.* (CUSB) Phys. Rev. **D46**, 1928 (1992).
[7] G. Crawford *et al.* (CLEO-II), Phys. Lett. **294B**, 139 (1992).
[8] Y. Kubota *et al.*, Nucl. Instrum. Meth. **A320**, 66 (1992).
[9] D. Peterson *et al.*, Nucl. Instrum. Meth. **A478**, 142 (2002).
[10] L. S. Brown and R. N. Cahn, Phys. Rev. **D13**, 1195 (1976).

[11] E. Barberio, B. van Eijk and Z. Was, Comput. Phys. Commun. **66**, 115 (1991); Comput. Phys. Commun. **79**, 291 (1994).
[12] We used $\mathcal{B}(\Upsilon(1S) \to l^+l^-) = 0.0243 \pm 0.0006$, $\mathcal{B}(\Upsilon(2S) \to l^+l^-) = 0.01245 \pm 0.0014$, which are averages of the $\mu^+\mu^-$ and e^+e^- world-average branching ratios [5].
[13] W. Kwong and J. L. Rosner, Phys. Rev. **D38**, 279 (1988).
[14] L. P. Fulcher, Phys. Rev. **D42**, 2337 (1990).
[15] W. Büchmuller, G. Grunberg and S.-H. Tye, Phys. Rev. Lett. **45**, 103 (1980); Phys. Rev. **D24**, 132 (1981).
[16] P. Moxhay and J. L. Rosner, Phys. Rev. **D28**, 1132 (1983).
[17] S. N. Gupta, S. F. Radford and W. W. Repko, Phys. Rev. **D34**, 201 (1986).
[18] S. N. Gupta, S. F. Radford and W. W. Repko, Phys. Rev. **D26**, 3305 (1982); Phys. Rev. **D30**, 2424 (1984).
[19] L. P. Fulcher, Phys. Rev. **D39**, 295 (1988).
[20] F. Daghighian and D. Silverman, Phys. Rev. **D36**, 3401 (1987).
[21] R. McClary and N. Byers, Phys. Rev. **D28**, 1692 (1983).
[22] E. Eichten, K. Gottfried, T. Kinoshita, K. D. Lane, and T. M. Yan, Phys. Rev. **D21**, 203 (1980).
[23] H. Grotch, D. A. Owen and K. J. Sebastian, Phys. Rev. **D30**, 1924 (1984).
[24] R. Barbieri, R. Gatto, R. Kogerler and Z. Kunszt, Phys. Lett. **B57**, 455 (1975); R. Barbieri, R. Gatto, and E. Remiddi, Phys. Lett. **B61**, 465 (1976); R. Barbieri, M. Caffo, and E. Remiddi, Nucl. Phys. **B162**, 220 (1980); W. Kwong, P. B. Mackenzie, R. Rosenfeld and J. L. Rosner, Phys. Rev. **D37**, 3210 (1988).
[25] I. C. Brock *et al.* (CLEO), Phys. Rev. **D43**, 1448 (1991).